JOURNAL OF SOLID STATE CHEMISTRY 60, 165–171 (1985)

Kinetics of Liquid–Solid Ion-Exchange Reactions of Transition Metal Ions in Tin(IV) Phosphate

PRITAM S. THIND AND JATINDER S. GANDHI

Department of Chemistry, Guru Nanak Dev University, Amritsar—143 005, India

Received October 2, 1984; in revised form April 16, 1985

A simple approach to liquid–solid ion exchange kinetics of Cu^{2+}, Zn^{2+}, Cd^{2+}, Co^{2+} ions in tin(IV) phosphate under different conditions of temperature, exchange ion concentration, and the particle size of the exchanger has been reported. The kinetics were controlled by particle diffusion and the $t^{1/2}$ law operated to about 65–75% of exchange. The diffusion coefficients and activation energies were calculated. The activation energies of Cu^{2+} and Co^{2+} ions were found to be low when compared with Zn^{2+} and Cd^{2+} ions due to Jahn–Teller distortion.

Introduction

Tin(IV) phosphate was first prepared by Merz (*1*) and he confirmed that this material had almost the same ion-exchange properties as amorphous zirconium phosphate. Subsequently, other workers prepared numerous gels by variation of preparative conditions (*2–4*). The phosphate tin ratio in the gels increased with increase of this ratio in the reactants. Inoue claimed that the limiting ratio was 5 : 4 and proposed a structure for this composition (*3*). However, the 5 : 4 ratio appears to be an artifact of his preparative condition.

Tin(IV) phosphate gels have been examined for possible use in the separation of fission products (*5–7*), and separations of ions have been carried out on papers impregnated with tin(IV) phosphate (*8, 9*). It has also been used as a support for the gas chromatographic separation of fatty acids (*10*). Crystallite tin(IV) phosphate has been prepared by heating the gels in 6 to 10 mole dm^{-3} phosphoric acid (*11–13*). Fuller assigned the formula $Sn(HPO_4)_2 \cdot nH_2O$ to the crystals. Crystalline tin(IV) phosphate apparently has a layered structure similar to that of α-ZrP (*14*). This conclusion is based on the similarities of their X-ray powder patterns (*11*) and the sorption of alkylammonium ions (*12*). Of the various studies on tin(IV) phosphate, the kinetics of ion exchange have received scant attention. The present kinetic study of Cu^{2+}, Zn^{2+}, Cd^{2+}, and Co^{2+} exchange has been made with tin(IV) phosphate in order to obtain information about the mechanism of diffusion of these ions.

Experimental

Tin(IV) phosphate was prepared by mixing tin(IV) tetrachloride pentahydrate (0.1 *M*) and ammonium dihydrogen phosphate (0.1 *M*) in the volume ratio of 1 : 1. The mix-

0022-4596/85 $3.00

FIG. 1. X-ray diffraction pattern on tin(IV) phosphate in Cu^{2+} form.

ing was done with constant sirring at 40°C. The pH of the final product was adjusted to 1.0 by adding either hydrochloric acid or alkali solution. The gel so obtained was kept for 24 hr and then it was filtered, followed by washings with distilled water until chloride ions were removed. Finally it was dried at 40°C and was converted to hydrogen form by treating with 0.1 *M* nitric acid for 24 hr with occasional shaking and intermittent changing of the acid. The product was washed with demineralized water in order to eliminate excess acid and was finally dried at 40°C and ground and sieved into three fractions (40/60, 60/80, and 80/100 mesh). The material was then converted to appropriate form. The physical and chemical characteristics of the prepared gel are: (a) the X-ray diffraction pattern (Fig. 1) shows the gel to be semicrystalline; (b) the chemical composition shows Sn : P as 5 : 2; (c) the cation exchange capacity is 0.92 meq/g. The 40/60 mesh fraction was used in all the experiments except in the study of the particle size effect when all the three size fractions were used. The exchanging electrolytes used were $Cu(NO_3)_2$, $Zn(NO_3)_2$, $Cd(NO_3)_2$, and $Co(NO_3)_2$.

Rates of exchange were determined by the limited bath technique (*15*). Solutions of copper, zinc, cadmium, and cobalt ions at constant ionic strength were thermostated at the required temperature in stoppered conical flasks, a weighed amount of the exchanger in hydrogen form (0.2 g) was added, and the flasks were thoroughly shaken. After appropriate intervals the contents of the flasks were filtered and Cu^{2+}, Zn^{2+}, Cd^{2+}, and Co^{2+} in the liquid phase were determined complexometrically with standard EDTA. The ion diffusion studies were conducted at 30, 40, and 50°C ± 1°C variation.

Results and Discussion

The rate-determining step of the ion exchange was ascertained by noting that the exchange rate was markedly dependent on the particle size of the exchanger, the rate increasing with decreasing particle size (Fig. 2). This clearly indicated a diffusion-controlled process and not one controlled by the chemical interaction of the exchanging ions because in the latter case the exchange rate would be independent of particle size. Distinction between particle diffusion and film diffusion was then made by: (a) the interruption test, showing that *F* versus time plots (Fig. 3) were discontinuous at the point of interruption, the exchange rate being higher immediately after the interruption than prior to it and establishing the exchange process to be particle-

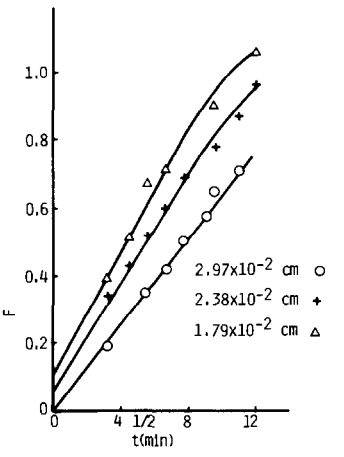

FIG. 2. Rate of Cd exchange in tin(IV) phosphate as a function of particle size.

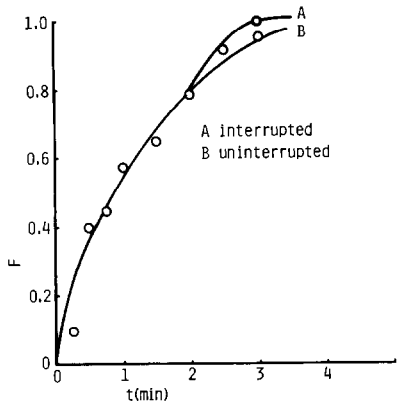

FIG. 3. Exchange of Cd^{2+} in tin(IV) phosphate with and without interruption.

diffusion-controlled; and (b) The nonlinear behavior of log(1-F) versus time plots (Fig. 4) indicating that the rate is governed neither by film diffusion nor by a mass action mechanism (*16*). The shapes of these plots, called McKay plots (*17*), are similar to those obtained for independent radioactive decay. The curves can be resolved (*18*) into two linear components. This indicates two interdiffusion processes: a faster one corresponding to the residual curve and a slower one corresponding to the later linear portion of the McKay plot, contributing to the overall rate of exchange. This observation is further confirmed by the shapes of F versus time plots (Fig. 5), which indicate that rapid initial uptake is followed by slower uptake of the effective ions. This suggests that the effective diffusion coefficient, in the present system, is comprised of two components which may be attributed to the simultaneous diffusion of the counterions through the pores of different size and electric fields. It is also clear from the residual curves that with the rise in temperature, the contribution of the faster component of the effective diffusion is increased. These observations are similar to those of Helfferich *et al.* (*19–22*), who explained the variable interdiffusion coefficients on the basis of electropotential gradient along the diffusion path. The following equation is valid for diffusion through the exchanger particles:

$$F = 1 - \frac{6}{\pi^2} \sum_{n=1}^{\infty} \frac{\exp(-n^2 Bt)}{n^2} \qquad (1)$$

where $B = \pi^2 \, Di/r^2$, r = radius of the parti-

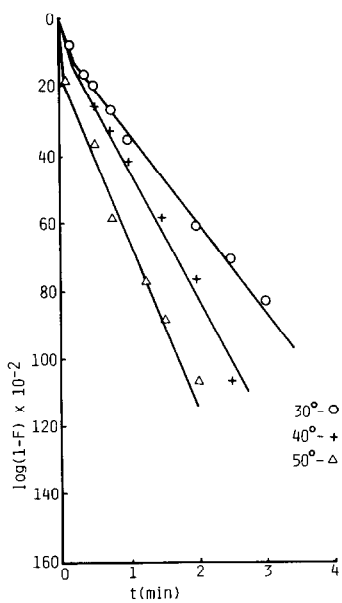

FIG. 4. McKay plot of log(1-F) vs time for Co^{2+} exchange in tin(IV) phosphate as a function of temperature.

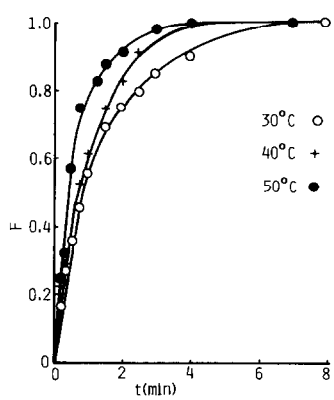

FIG. 5. Rate of exchange of Co^{2+} at different temperature on tin(IV) phosphate.

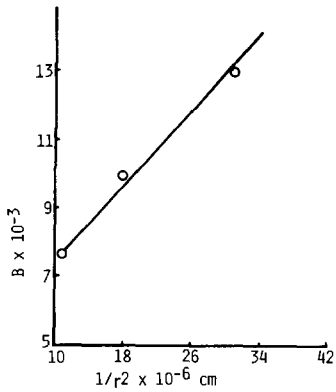

FIG. 6. B as a function of $1/r^2$.

cle, and Di = effective diffusion coefficient of the two ions undergoing exchange within the exchanger. The plot of the diffusion rate constant B against $1/r^2$ (Fig. 6) is linear, and the linearity of the dependence also confirms that diffusion within the particles is the step which controls the exchange rate.

Quantitative formulation of the exchange kinetics was done by applying the particle diffusion equation observed (*23*) for zeolite exchangers, viz. $Q_t/Q_\infty = (2A/V)(\mathrm{Di}\ t/\pi)^{1/2}$, where Q_t and Q_∞ are the amounts of exchange at time t and at equilibrium, respectively, A and V are the surface area and volume of the exchanger particles, and Di is the effective or apparent diffusion coefficient. In the case of spherical particles of radius r, the above relation becomes

$$F = \frac{Q_t}{Q_\infty} = \frac{6}{r}\left(\frac{\mathrm{Di}\ t}{\pi}\right)^{1/2} \qquad (2)$$

To test the validity of Eq. (1), the values of Q_t/Q_∞ were plotted against $t^{1/2}$ for each concentration of the exchanging electrolytes. The plots, some of which are shown in Fig. 2, were linear in the initial stages up to 65–75% exchange, showing that exchange kinetics followed the particle diffusion mechanism. (In Fig. 2 the axes of the individual plots have been shifted gradually as shown, the axial divisions remaining the same.) The diffusion coefficients calculated from the slopes of the plots are given in Table I. It is seen from Table I that the diffusion coefficient for a particular concentration increased with an increase in temperature. This is in conformity with the fact that the exchange diffusion coefficient generally increases with temperature (*24–25*). The diffusion coefficients also increased with increasing concentration, which might be due to the increased co-ion concentration (*26*) when the external counterion concentration was increased.

In order to explain the observed variation of diffusion coefficients of the different exchanging cations, attempts were made to correlate the diffusion coefficients with the radius of the ingoing cations. The diffusivity of the exchange cations in the negatively charged tin(IV) phosphate matrix depends on the above-mentioned parameter as shown in Fig. 7.

Activation energies were calculated from the slopes of the plots, some of which are shown in Fig. 8, with the help of an Arrhenius-type equation:

TABLE I

DIFFUSION COEFFICIENTS OF ION EXCHANGE IN TIN(IV) PHOSPHATE AS A FUNCTION OF TEMPERATURE, CONCENTRATION, AND PARTICLE SIZE

Cation	Temperature (K)	Di (10^7 cm^2 sec^{-1})	Cation	Concentration (mole liter^{-1})	Di (10^7 cm^2 sec^{-1})	Cation	Particle size (10^{-2} cm)	Di (10^7 cm^2 sec^{-1})
Zn^{2+}	303	4.22	Zn^{2+}	0.0184	3.24	Cd^{2+}	2.97	3.84
Zn^{2+}	313	9.39	Zn^{2+}	0.0478	4.81	Cd^{2+}	2.38	4.51
Zn^{2+}	323	13.18	Zn^{2+}	0.0988	5.03	Cd^{2+}	1.79	6.00

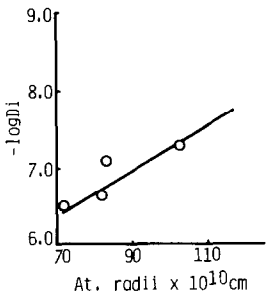

FIG. 7. Di as a function of atomic radius.

$$\log \mathrm{Di} = \mathrm{const} - \frac{E}{4.576T}$$

where E is the activation energy for diffusion and T is the absolute temperature. The striking difference between the activation energy of Co^{2+} and Cu^{2+} from Zn^{2+} and Cd^{2+} (Table II) can be explained on the basis of the electronic configuration of these $3d$ transition metal ions. Thus ligand field theory provides ample evidence of differences between a $3d^7$ ion as Co^{2+}, $3d^9$ ion as Cu^{2+}, and $3d^{10}$ ions as Zn^{2+} or Cd^{2+}. The crystal field stabilization energies for octahedrally and tetrahedrally coordinated Zn^{2+} and Cd^{2+} do not differ. The $3d^7$ Co^{2+} and $3d^9$ Cu^{2+}, however, have a higher octahedral than tetrahedral stabilization energy. This

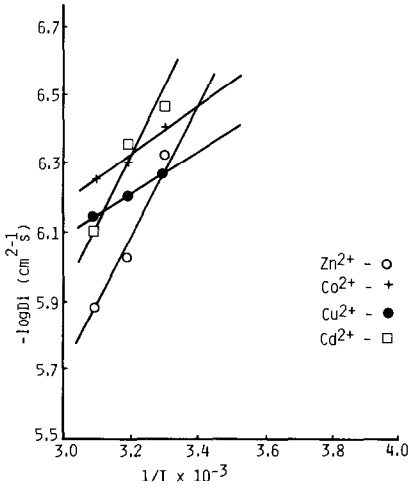

FIG. 8. Log Di against $1/T$ (K).

TABLE II

SELF-DIFFUSION COEFFICIENTS AND ENERGY OF ACTIVATION OF Cu^{2+}, Co^{2+}, Zn^{2+} AND Cd^{2+} ON TIN(IV) PHOSPHATE

Cations	Do (10^7 cm^2 sec^{-1})	E (kcal deg^{-1} mole^{-1})
Cu^{2+}	3.25	2.7
Co^{2+}	2.20	3.1
Zn^{2+}	0.81	9.1
Cd^{2+}	0.51	11.0

difference in the stabilization energies of the ions does not mean that Co^{2+} and Cu^{2+} can only coordinate octahedrally. However, if we suppose that $Co(H_2O)_6^{2+}$, $Cu(H_2O)_6^{2+}$, $Zn(H_2O)_6^{2+}$ and $Cd(H_2O)_6^{2+}$ ions enter the exchanger framework with loss of some water of hydration and then coordinate the negative oxygen ligands of the lattice, it is doubtful if the initial octahedral configuration can be preserved after entering into the exchange phase. If we compare the lability of water molecules in the case of $Co(H_2O)_6^{2+}$ and $Cu(H_2O)_6^{2+}$ with that of $Zn(H_2O)_6^{2+}$ and $Cd(H_2O)_6^{2+}$ then it is more in the former case due to Jahn–Teller distortion which leads to the easy diffusion of these hydrated ions into the exchanger phase because H_2O in these ions can be easily replaced by negative oxygen ligands of the lattice. Therefore the activation energy in the case of Zn^{2+} and Cd^{2+} is greater when compared with Co^{2+} and Cu^{2+} ions. It would be pertinent here to compare the activation energy for diffusion in the synthetic tin(IV) phosphate under present study with those found with organic exchangers and natural zeolites. The activation energies for the different cations as studied here were in the range 2–11 kcal/g-ion (Table II), whereas for organic exchangers and zeolites the activation energies vary in the range 5–10 (*27*) and 10–30 (*25*) kcal/g-ion, respectively. For the ion exchange process, the observed activation energy barrier corresponds to that for the combination of the

tin(IV) phosphate framework and the enclosed pore liquid which is in aqueous solution of the exchange cations. The activation energy for electrolytic conductance, and hence for ionic migration in aqueous medium, is about 3.6 kcal (*28*) for most ions. As the average activation energy for diffusion in the present work is 6.50 kcal/mole, the diffusion barrier of the tin(IV) phosphate framework comes to about 2.90 kcal/mole for the divalent cations studied. This is a very rough estimation as the value 3.60 kcal, which is valid for infinitely dilute solutions, should be somewhat modified when applied to the pore liquid because of ion–ion interactions.

It is seen from Fig. 2 that the relative exchange rate in the initial period increased with decreasing particle size of the exchanger. This was obviously due to the increase in specific surface as it is through the solution–solid interface that the exchange actually takes place. However, the diffusion coefficient of the exchanging ion should not vary with the particle size of the exchanger as the diffusion coefficient is defined in terms of unit area of the surface through which diffusion occurs. However, it is seen from Table I that the diffusion coefficient of the counterion actually decreased with a decrease in the particle size of the exchanger. This abnormal behavior may be explained as follows: In the larger particles of the exchanger there should occur an appreciable number of microcracks (introduced by the crushing operation on still larger lumps) in addition to the molecular channels present in the structure itself. Diffusion in such particles would therefore occur not only through the channels but through the cracks as well. Consequently, the diffusion rate, and hence the apparent diffusion coefficient, would be higher than it would be for the molecular channels alone. However, as the particles are progressively reduced in size, the microcracks would be gradually eliminated by fractures occurring at the cracks, and hence the additional diffusion through the cracks would gradually disappear, leaving only channel diffusion in the smallest size particles. Hence the apparent diffusion coefficient, which is the result of the effects of crack diffusion and channel diffusion, would gradually decrease as the particle size of the exchanger is reduced.

Acknowledgments

The authors are grateful to Professor Harjit Singh for providing research facilities. One of us (JSG) also thanks the UGC, New Delhi for financial assistance.

References

1. E. MERZ, *Z. Electrochem.* **63,** 288 (1959).
2. Y. INOUE, *J. Inorg. Nucl. Chem.* **26,** 2241 (1964).
3. Y. INOUE, *J. Bull. Chem. Soc. Japan* **36,** 1316 (1963).
4. J. PIRET, J. HENRY, G. BALON, AND C. BEAUDT, *Bull Soc. Chim. France,* 3590 (1965).
5. Y. INOUE, *Bull. Chem. Soc. Japan* **36,** 1324 (1963).
6. Y. INOUE, S. SUZUKI, AND H. GETO, *Bull. Chem. Soc. Japan* **37,** 1547 (1964).
7. A. SATO, Y. INOUE, AND S. SUZUKI, *Bull. Chem. Soc. Japan* **39,** 716 (1966).
8. M. QURESHI AND S. Z. QURESHI, *J. Chromatogr.* **22,** 198 (1966).
9. C. C. CHANG, *Hua Hsueh Hsueh Pao* **31,** 571 (1965).
10. K. KONICHI AND Y. LANE, *Bunseki Kagaku* **13,** 299 (1964).
11. A. WINKLER AND E. THILO, *Z. Anorg. Allg. Chem.* **346,** 92 (1966).
12. E. MICHEL AND A. WEISS, *Z. Naturforsch. B* **22,** 1100 (1967).
13. M. J. FULLER, *J. Inorg. Nucl. Chem.* **33,** 559 (1971).
14. A. CLEARFIELD AND G. DAVID SMITH, *Inorg. Chem.* **8,** 431 (1969).
15. J. P. RAWAT AND P. S. THIND, *J. Phys. Chem.* **80,** 1384 (1976).
16. CARLA HEITNER-WIRGUIN AND G. MARKOVITS, *J. Phys. Chem.* **67,** 2263 (1963).
17. H. MCKAY, *Nature (London)* **142,** 997 (1938).
18. G. FRIEDLANDER AND J. W. KENNEDY "Nuclear and Radiochemistry," p. 128, Wiley, New York (1956).

19. R. SCHLOGL AND F. HELFFERICH, *J. Chem. Phys.* **26,** 5 (1957).
20. F. HELFFERICH AND M. S. PLESSET, *J. Chem. Phys.* **28,** 418 (1958).
21. M. S. PLESSET, F. HELFFERICH, AND J. N. FRANKLIN, *J. Chem. Phys.* **29,** 1064 (1958).
22. F. HELFFERICH, *J. Chem. Phys.* **66,** 39 (1962).
23. R. M. BARRER AND L. HINDS, *J. Chem. Soc.*, 1879 (1953); R. M. BARRER AND J. D. FALCONER, *Proc. R. Soc. London Ser. A* **236,** 227 (1956).
24. F. HELFFERICH "Ion-Exchange," Chapt. 6, McGraw–Hill, New York (1962).
25. R. M. BARRER, *Proc. Chem. Soc.*, 99 (1958).
26. R. SCHLOGL, *Z. Elektrochem.* **57,** 195 (1953).
27. G. E. BOYD AND B. A. SALDANO, *J. Amer. Chem. Soc.* **75,** 6091 (1953); G. E. BOYD, B. A. SALDANO, AND O. D. BONNER, *J. Phys. Chem.* **58,** 456 (1954).
28. S. GLASSTONE, "An Introduction to Electrochemistry," p. 62, Van Nostrand Affiliated East-West Press Pvt. Ltd., New Delhi (1965).